Phenomenological theory of bistability in polariton diodes

Daniele Bajoni,[1] Elizaveta Semenova,[2,a)] Aristide Lemaître,[2] Sylvain Barbay,[2] Robert Kuszelewicz,[2] and Jacqueline Bloch[2,b)]
[1]*CNISM UDR Pavia and Dipartimento di Elettronica, Università degli studi di Pavia, via Ferrata 1, 27100 Pavia, Italy*
[2]*CNRS-Laboratoire de Photonique et Nanostructures, Route de Nozay, 91460 Marcoussis, France*

(Received 14 May 2010; accepted 4 July 2010; published online 2 September 2010)

Polariton diodes have been recently shown to exhibit pronounced bistability induced by the control of the light-matter coupling via an external bias and optical pumping [D. Bajoni, E. Semenova, A. Lemaître, S. Bouchoule, E. Wertz, P. Senellart, S. Barbay, R. Kuszelewicz, and J. Bloch, Phys. Rev. Lett. **101**, 266402 (2008)]. In the present paper, we detail the phenomenological theory developed to describe the observed hysteresis cycles and present additional experimental data confirming the validity of the present model. © *2010 American Institute of Physics*. [doi:10.1063/1.3481693]

Bistability is a fascinating property of nonlinear systems in which the measure of a physical quantity (for instance the optical transmission of a sample[1] or the resistivity of a diode[2]) may give different results depending of the history of the system. This capability to keep track of the previous state of a measurable quantity has been widely investigated to realize ultrafast memories in electronical[3] and optical circuits.[4] In the optical domain much interest has been devoted to bistability in recent years as an effective mean to achieve all-optical signal processing.[4–6]

Microcavity polaritons are exciton-photon hybrid states originating from the strong coupling regime between excitons confined in quantum wells (QWs) and the photonic mode of an optical microcavity.[7] It has been shown that polaritons can be electrically controlled by doping the Bragg mirrors of the microcavity (polariton diodes[8–10]), so that the amplitude of the electrical field ($\mathcal{E}$) in the QWs can be set using an external bias (V_B). We have recently shown that polariton diodes can undergo low-power optical bistability based on the strong (SC) to weak (WC) coupling passage; such passage is due to exciton ionization because of the pulling force of $\mathcal{E}$ on electrons and holes and can thus be tuned via V_B.[11] In this paper we detail an analytical model introduced in Ref. 11 which has allowed describing the observed bistability and present additional experimental data.

Bistability experiments rely on experimental configurations as that shown in Fig. 1(a): the polariton diode cooled down to 10 K is polarized in reverse by V_B, the circuit is closed on a load resistance Z, and a laser excites the sample at a well defined energy. The sample (described in detail in Ref. 8) was grown by molecular beam epitaxy on an n-doped GaAs substrate. It consists of an undoped GaAs cavity containing three $In_{0.05}Ga_{0.95}As$ QWs and surrounded by a p-doped and an n-doped $Ga_{0.9}Al_{0.1}As/Ga_{0.1}Al_{0.9}As$ Bragg mirror. Square mesas of 300 μm lateral size were etched down to the GaAs substrate and connected with metal contacts. When the polariton diode is reverse biased, a large hysteresis cycle is observed under resonant optical excitation, both when sweeping the optical power or the bias voltage: the physical origin of the bistability is the strong variation in the exciton coherence time with the intra-cavity electric field.

To understand the observed bistability we need to calculate the optical response of the system as a function of the exciton coherence time τ_X (the coherence time of the cavity mode does not change during the considered experiments). Transmission spectra of the cavity sample are calculated using the transfer matrix method,[12] using for the exciton resonance the index of refraction calculated in Ref. 13. Transmission spectra for various values of τ_X [Fig. 1(b)] were calculated using parameters corresponding to the sample of Ref. 8: the spectra correctly simulate the experimental linewidths and Rabi splitting. For small values of τ_X, the system is in weak coupling and the only resonance is the fundamental mode of the cavity. The passage to strong coupling occurs when τ_X becomes longer than $1/\Omega$ where $\hbar\Omega=5$ meV is the Rabi splitting.[7] When in strong coupling the sample presents two resonances (the upper and lower polariton[7]) separated by

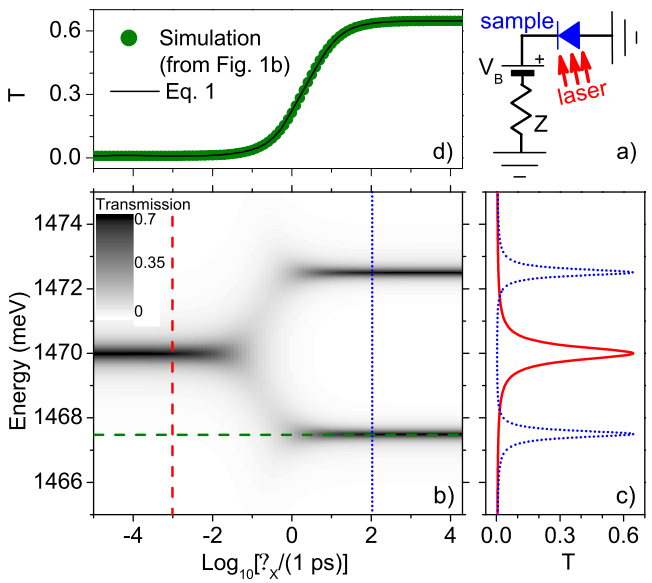

FIG. 1. (Color online) (a) Scheme of the experiment. (b) Calculated transmission (gray scale) of the sample as a function of τ_X. (c) Calculated transmission curves for weak coupling [red solid line, corresponding to the red dashed vertical line in panel (b)] and strong coupling [blue dotted line, corresponding to the blue dotted vertical line in panel (b)]. (d) Profile of the transmission dependence on τ_X extracted from the simulations [green dots, corresponding to the green dashed horizontal line in panel (b)] and its best fit with Eq. (1) (solid red line).

a)Now at the Department of Photonics Engineering, Technical University of Denmark, Orsteds Plads, DK 2800 Kgs. Lyngby, Denmark.
b)Electronic mail: jacqueline.bloch@lpn.cnrs.fr.

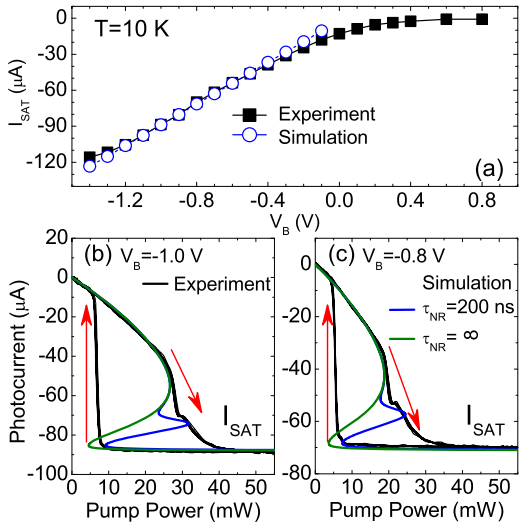

FIG. 2. (Color online) (a) Experimental (black dots) and calculated (blue dots) dependence of the saturation current on the external bias. [(b) and (c)] Experimental (black line) and calculated (blue and green lines) bistable cycle for $V_B=-1.0$ V (b) and $V_B=-0.8$ V (c). The blue line is for $\tau_{NR}=200$ ns while the green line is for $\tau_{NR}=\infty$.

a few meV. This change in the photonic density of states can be used to obtain bistability:[11,14] if the laser is tuned to one of the polariton branches τ_X depends on the pump intensity, and the passage from weak to strong coupling abruptly modifies the laser transmission, providing the positive feedback loop necessary for bistability.

We now consider an optical excitation with a laser tuned to the energy of the lower polariton branch. The simulated cavity transmission (T) at this energy is shown as green dots in Fig. 1(d) as a function of τ_X: it strongly varies as the system transits from weak to strong coupling regime. In order to implement this results in an analytic model, an analytic expression for T is needed: as shown by the red line in Fig. 1(d), the evolution of the transmission with τ_X can be perfectly described using the formula, as follows:

$$T = T_{SC} + \frac{T_{WC} - T_{SC}}{1 + 0.474\tau_X}, \tag{1}$$

where SC (WC) refers to the strong (weak) coupling, $T_{WC}=0.01$, $T_{SC}=0.65$, τ_X must be expressed in picosecond. In the experiments of Ref. 11, the laser beam was shone on a 50 μm spot and has a divergence of 10°: when the sample is in SC only the part of the beam around 0° is absorbed due to the filtering properties of the polariton resonance, and therefore, T_{SC} has to be reduced to 0.02.

Three main terms contribute to τ_X: the scattering with phonons [with characteristic time $\tau_{X0}=10$ ps (Ref. 15)] and the tunneling of electrons and holes out of the QW due to the drag of the *mathcal E*, as follows:

$$\tau_X = \left(\frac{1}{\tau_{X0}} + \frac{1}{\tau_{t,e}} + \frac{1}{\tau_{t,h}}\right)^{-1}. \tag{2}$$

The tunneling time of electrons and holes ($\tau_{t,e}$ and $\tau_{t,e}$) out of the quantum well are dependent on the electric field $\mathcal{E}$:[16]

$$\tau_{t,(e,h)} = \frac{2m^*_{e,h}L^2_{QW}}{\hbar\pi}\exp\left(\frac{4}{3\hbar e\mathcal{E}}\sqrt{2m^*_{e,h}U^3_{e,h}}\right), \tag{3}$$

where $m^*_{e,h}$ and $U_{e,h}$ are respectively the reduced masses and binding energies of electrons and holes ($U_e=42$ meV, $U_h=5$ meV for the QW in Ref. 11) and $L_{QW}=8$ nm is the width of the QW.

Applying the second Kirchoff law to the circuit of Fig. 1(a), $\mathcal{E}$ is given by:

$$\mathcal{E} = \frac{\phi - V_B + ZI}{L_{CAV}}, \tag{4}$$

where ϕ is the built-in potential, $L_{CAV}=236$ nm the width of the cavity,[8] Z the measured load resistance [Fig. 1(a)] and I the photocurrent which we now want to evaluate. Each photon entering the cavity has a probability η of being absorbed creating an exciton (or a polariton, in SC) which in turn has a probability $1/\tau_{rad}$ to recombine radiatively. There is also a probability $1/\tau_{t,(e,h)}$ of carrier tunneling out of the QW. Thus,

$$\frac{dn_X}{dt} = \eta T\frac{P}{E_L} - \frac{n_X}{\tau_{rad}} - \frac{n_X}{\tau_{t,e}} - \frac{n_X}{\tau_{t,h}},$$

$$\frac{dn_e}{dt} = \frac{n_X}{\tau_{t,h}} - \frac{n_e}{\tau_{t,e}} - \frac{n_e}{\tau_{NR}},$$

$$\frac{dn_h}{dt} = \frac{n_X}{\tau_{t,e}} - \frac{n_h}{\tau_{t,h}}, \tag{5}$$

where $n^{e,h}$ are the populations of unbound electrons and holes and n_X the exciton population, P is the pump power and $E_L=1467.5$ meV is the energy of the lower polariton resonance. We neglect bimolecular recombination of electron and holes Bn_en_h (Ref. 17) and bimolecular formations of excitons Cn_en_h,[18] because they have much longer time scales than $\tau_{t,(e,h)}$ and τ_{rad}. The time $\tau_{NR}=200$ ns accounts for the nonradiative recombination of electrons (see discussion below). Both η and τ_{rad} take different values in the strong and weak coupling regime, and a similar functional as in Eq. (1) has been used to describe their dependence on $\mathcal{E}$. In weak coupling $\tau^{WC}_{rad}=1$ ns corresponds to the radiative recombination time of excitons[19] and η_{WC} is the QW absorption: the data are best fitted for $\eta_{WC}=0.02$, a value fully consistent for $In_{0.05}Ga_{0.95}As$ QWs;[20] this is, along with τ_{NR} (see below), the only fitting parameter. In the strong coupling regime $\eta_{SC}=1$, as all photons entering the cavity become polaritons,[7] and $\tau^{SC}_{rad}=2$ ps is the radiative recombination time of polaritons.[7] Finally, I is the sum of the electron and hole currents

$$I = -e\left(\frac{n_X}{\tau_{t,e}} + \frac{n_e}{\tau_{t,e}} + \frac{n_X}{\tau_{t,h}} + \frac{n_h}{\tau_{t,h}}\right)$$
$$= -\frac{\eta TeP}{E_L}\frac{\tau_{rad}[\tau^2_{t,e} + 2\tau_{t,h}\tau_{NR} + 2\tau_{t,e}(\tau_{t,h} + \tau_{NR})]}{(\tau_{t,e} + \tau_{NR})[\tau_{t,h}\tau_{rad} + \tau_{t,e}(\tau_{t,h} + \tau_{rad})]}, \tag{6}$$

where the second line is obtained by solving Eq. (5) under steady state conditions ($dn_X/dt = dn_e/dt = dn_h/dt = 0$).

Equation (6) implicitly defines the function $I(P)$: the quantities η, T, τ_{rad}, and $\tau_{t,(e,h)}$ on its right hand side actually depend on $\mathcal{E}$ and thus on the photocurrent through Eq. (4). One parameter that needed to be adjusted to describe the experimental data is the built-in potential ϕ. To determine this value, we consider excitation conditions where the sample is in strong coupling regime and approaches the flat-band condition ($\mathcal{E}\to 0$). Then the photocurrent saturates to the value exactly compensating the external bias and built-in potential: $I_{SAT}=(V_B-\phi)/Z$.

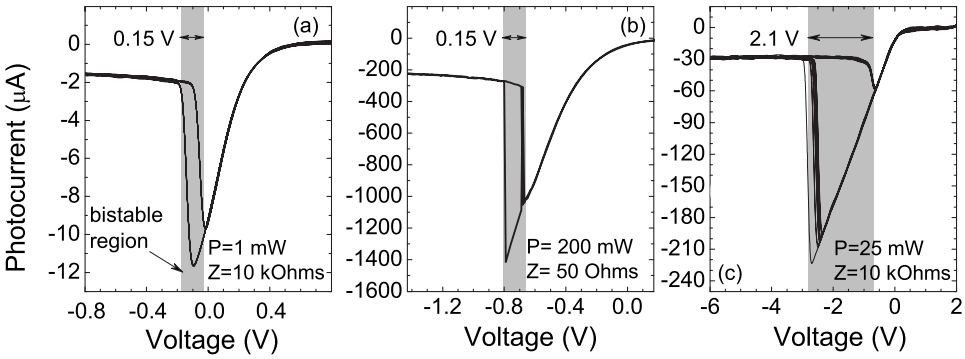

FIG. 3. (a) Experimental photocurrent hysteresis cycles measured varying V_B for a) P=1 mW and Z=10 kΩ; (b) P=200 mW and Z=50 Ω and (c) P =25 mW and Z=10 kΩ.

Experimental values of I_{SAT} are plotted in Fig. 2(a) as a function of V_B: for $-1.5\ \text{V} < V_B < 0$, I_{SAT} varies linearly as expected from our phenomenological model which gives $\phi = 0.07$ V. Using this value, two examples of calculated bistability curves, compared to the experiment, are shown in Figs. 2(b) and 2(c) in blue. There is good agreement between theory and experiment, in particular the slope of the photocurrent in the photovoltaic region near zero, and the optical powers of the forward and backward switch of state (highlighted with red arrows). Notice also that, during the switch between weak and strong coupling, a small bump appears in the photocurrent which corresponds, in the fits, by a turn of the curve toward high P. This turn occurs in a regime in which $\tau_{NR} \ll \tau_{t,e} \ll \tau_{t,h}$ and nonradiative recombination of electrons sweeps away carriers thus reducing the photocurrent. This is confirmed by fitting the experimental data by using $\tau_{NR} = \infty$ in Eq. (5) as shown by the green curves in Figs. 2(b) and 2(c): without nonradiative recombination the described feature disappears. A good fit of the experimental data is obtained for $\tau_{NR} = 200$ ns.

Such satisfactory fits of the experimental curves could be obtained only for $-1.5\ \text{V} < V_B < 0$. Notice that the value we use for the built-in potential is far from 1.48 V, the expected value in GaAs for the present doping levels.[21] These discrepancies can possibly be due to charge accumulation in the doped mirrors of the microcavity, which cannot be accounted for in this model. One of the most compelling features of this model is that the bistability depends on the external feedback of the load resistance Z, through the ZI term in Eq. (4).

This point is confirmed by the experiments: in Fig. 3, experimental bistability curves are shown in which $\mathcal{E}$ is controlled by changing V_B while P remains constant. The width of the hysteresis cycles in Figs. 3(a) and 3(b) have roughly the same extent of 0.15 V, even if P differs by more than two orders of magnitude. However notice that in both cases, the product $P \cdot Z$ remains the same. This is consistent with the fact that P enters the model multiplied to Z, in Eqs. (4) and (6). In comparison, a pump power of 25 mW is sufficient to obtain a much larger (~2.1 V) bistable region with $Z = 10$ kΩ, as shown in Fig. 3(c).

In summary we have presented a phenomenological model used to explain optical bistability in electrical circuits involving polariton diodes. The model describes the interplay between the photocurrent flowing to the circuit and the optical response of the sample. Some discrepancies remain between the model and the experimental data: a full microscopic description, solving the equations of transport in semiconductors[21] in parallel to optical propagation in each layer would be necessary for complete agreement. Regardless of its simplicity the present model fits experimental curves with accuracy and gives a good overall understanding of the underlying physics; it could be applied as a tool to design bistable polariton devices.

This work was funded by C'nano Ile de France and Conseil Général de l'Essonne. We acknowledge CNISM support through the "Innesco" initiative and the European Community for funding through the Marie Curie project ÒClermont 2Ó under Contract No. MRTN-CT-2003-503677. We thank Sophie Bouchoule and Pascale Senellart for fruitful discussions.

[1] H. M. Gibbs, S. L. McCall, and T. N. C. Venkatesan, Phys. Rev. Lett. **36**, 1135 (1976).
[2] V. J. Goldman, D. C. Tsui, and J. E. Cunningham, Phys. Rev. Lett. **58**, 1256 (1987).
[3] S. Y. Chung, N. Jin, P. R. Berger, R. Yu, P. E. Thompson, R. Lake, S. L. Rommel, and S. K. Kurinec, Appl. Phys. Lett. **84**, 2688 (2004).
[4] H. M. Gibbs, *Optical Bistability: Controlling Light With Light* (Academic, New York, 1985).
[5] V. R. Almeida, C. A. Barrios, R. R. Panepucci, and M. Lipson, Nature **431**, 1081 (2004).
[6] V. R. Almeida and M. Lipson, Opt. Lett. **29**, 2387 (2004).
[7] M. S. Skolnick, T. A. Fisher, and D. M. Whittaker, Semicond. Sci. Technol. **13**, 645 (1998).
[8] D. Bajoni, E. Semenova, A. Lematre, S. Bouchoule, E. Wertz, P. Senellart, and J. Bloch, Phys. Rev. B **77**, 113303 (2008).
[9] A. A. Khalifa, A. P. D. Love, D. N. Krizhanovskii, M. S. Skolnick, and J. S. Roberts, Appl. Phys. Lett. **92**, 061107 (2008).
[10] S. I. Tsintzos, N. T. Pelekanos, G. Konstantinidis, Z. Hatzopoulos, and P. G. Savvidis, Nature (London) **453**, 372 (2008).
[11] D. Bajoni, E. Semenova, A. Lemaître, S. Bouchoule, E. Wertz, P. Senellart, S. Barbay, R. Kuszelewicz, and J. Bloch, Phys. Rev. Lett. **101**, 266402 (2008).
[12] A. Yariv and P. Teh, *Optical Waves in Crystals* (Wiley, New York, 1984).
[13] L. C. Andreani and A. Pasquarello, Phys. Rev. B **42**, 8928 (1990).
[14] M. Gurioli, L. Cavigli, G. Khitrova, and H. M. Gibbs, Semicond. Sci. Technol. **19**, S345 (2004).
[15] H. Stolz, D. Schwarze, W. von der Osten, and G. Weimann, Superlattices Microstruct. **9**, 511 (1991).
[16] G. Bastard, J. A. Brum, and R. Ferreira, *Solid State Physics* (Academic, New York, 1991), Vol. 44, p. 229.
[17] T. Matsusue and H. Sakaki, Appl. Phys. Lett. **50**, 1429 (1987).
[18] C. Piermarocchi, F. Tassone, V. Savona, A. Quattropani, and P. Schwendimann, Phys. Rev. B **55**, 1333 (1997).
[19] L. V. Dao, M. B. Johnston, M. Gal, L. Fu, H. H. Tan, and C. Jagadish, Appl. Phys. Lett. **73**, 3408 (1998).
[20] R. Atanasov, F. Bassani, A. D'Andrea, and N. Tommasini, Phys. Rev. B **50**, 14381 (1994).
[21] Bart Van Zeghbroeck, "Principles of Semiconductor Devices," http://ecee.colorado.edu/bart/book/.